Bragg Interaction of Electromagnetic Waves in a Ferrite Slab Periodically Loaded with Metal Strips

CHARRAY SURAWATPUNYA, MAKOTO TSUTSUMI, MEMBER, IEEE, AND NOBUAKI KUMAGAI, FELLOW, IEEE

Abstract—**The waveguiding characteristics of electromagnetic TE waves in a ferrite slab periodically loaded with metal strips are investigated. Theoretical formulation by means of the spectral domain approach is employed to obtain the Brillouin diagrams of two types of volume modes and a surface mode. It is found that the nonreciprocal properties of waves depend on the metal strip profile and bias magnetic field strength. Experiments on the magnetic-field dependence of the Bragg frequency and the stop bandwidth are carried out in the millimeter-wave frequencies. Typical results obtained from a polycrystalline YIG slab with periodic gold strips deposited on one surface are: stop bandwidth about 2.14 GHz, with return loss about 2 dB at the Bragg frequency of 47.5 GHz, for the bias magnetic-field strength of 5.7 kG. The Bragg frequency can be tuned over the range of 1.39 GHz by varying the bias magnetic field from 0 to 8.2 kG. Experimental results show good agreement with theoretical predictions.**

I. Introduction

RECENTLY, MANY research works have been done in connection with ferrite periodic structures for microwave and millimeter-wave applications. Tsutsumi *et al.* [1] have studied the Bragg reflection of millimeter waves by a corrugated ferrite slab and have found that the tunable property of the Bragg frequency by the applied magnetic field is useful in designing tunable band-rejection filters. With application to a beam-steerable leaky-wave antenna in mind, Ohira *et al.* [2] have investigated the radiation of a leaky wave from a grooved ferrite image line and have demonstrated experimentally that the radiation angle of the leaky wave can be steered continuously by the dc-bias magnetic field. Araki *et al.* [3] have studied the nonreciprocal leakage phenomena in the grating ferrite waveguides. They have shown that these leakage phenomena can be used to develope new planar isolators and circulators.

In the present paper, the propagation characteristics of electromagnetic TE waves in the ferrite slab with periodic metal strips are investigated. The spectral domain approach, which was followed by Ogusu [4] in the study of propagation properties of a dielectric waveguide with periodic metal strips, is employed to obtain the Brillouin diagrams of this type of periodic structure. Brillouin diagrams around the first-order Bragg interaction region are shown numerically for two volume and one surface modes. Stopband properties as a function of strip width and applied magnetic field are determined and compared with the experimental results carried out in the frequency range 40–50 GHz using polycrystalline YIG slabs periodically loaded with copper or gold strips. The nonreciprocal behavior of waves due to the periodic perturbation of metal strips in the waveguide structure is also discussed briefly.

Manuscript received October 28, 1983; revised February 9, 1984.

C. Surawatpunya was with the Department of Electrical Communication Engineering, Osaka University, Yamada Oka, Suita, Osaka 565, Japan. He is now with King Mongkut's Institute of Technology, Ladkrabang Campus, Ladkrabang, Bangkok, Thailand.

M. Tsutsumi and N. Kumagai are with the Department of Electrical Communication Engineering, Osaka University, Yamada Oka, Suita, Osaka 565, Japan.

II. Theoretical Formulation

Fig. 1 shows the structure of the ferrite slab periodically loaded with infinitesimally thin metal strips of width s at an interval d. The structure is assumed to be uniform and infinite in the bias dc magnetic-field direction. Hence, the fields have no variation in the z direction. It is also assumed that the guided waves propagate in the y direction with time dependence $\exp(j\omega t)$. The permeability tensor of the ferrite slab is given by [5]

$$[\hat{\mu}] = \begin{bmatrix} \mu & j\kappa & 0 \\ -j\kappa & \mu & 0 \\ 0 & 0 & 1 \end{bmatrix} \tag{1}$$

where

$$\mu = 1 + \frac{(\gamma\mu_0)^2 M H_0}{(\gamma\mu_0 H_0)^2 - \omega^2}, \qquad \kappa = \frac{(\gamma\mu_0) M \omega}{(\gamma\mu_0 H_0)^2 - \omega^2}$$

γ, M, and H_0 are the gyromagnetic ratio, the saturation magnetization, and the bias-dc magnetic field, respectively. All of the materials are assumed to be lossless. We shall restrict ourself to the TE mode with field components H_x, H_y, and E_z, because only the TE mode is sensitive to the applied magnetic field for a two-dimensional problem [6]. From Maxwell's equations, the E_z component inside the ferrite slab satisfies the following differential equation:

$$\left(\frac{\partial^2}{\partial x^2} + \frac{\partial^2}{\partial y^2} + \omega^2 \mu_0 \epsilon_0 \epsilon_r \mu_{ef} \right) E_z = 0. \tag{2}$$

The H_x and H_y components can be easily expressed in

0018-9480/84/0700-0689$01.00 ©1984 IEEE

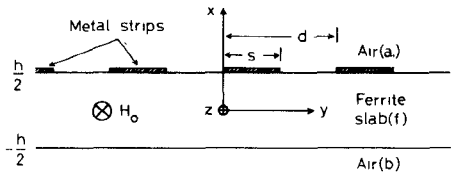

Fig. 1. Geometry of the ferrite slab with periodic metal strips.

terms of E_z from Maxwell's equations as

$$H_x = \frac{-1}{j\omega\mu_0}\left(\frac{j}{\kappa_{ef}}\frac{\partial}{\partial x}E_z + \frac{1}{\mu_{ef}}\frac{\partial}{\partial y}E_z\right) \tag{3}$$

$$H_y = \frac{-1}{j\omega\mu_0}\left(\frac{-1}{\mu_{ef}}\frac{\partial}{\partial x}E_z + \frac{j}{\kappa_{ef}}\frac{\partial}{\partial y}E_z\right) \tag{4}$$

where

$$\mu_{ef} = \frac{\mu^2 - \kappa^2}{\mu}, \qquad \kappa_{ef} = \frac{\mu^2 - \kappa^2}{\kappa}$$

and ϵ_r is the relative dielectric constant of the ferrite slab.

The theoretical analysis by means of the spectral domain approach [4] will be followed to derive the dispersion relation of the waveguide structure shown in Fig. 1. According to the Floquet's theorem, we shall expand the E_z component in the ferrite and air in terms of space harmonics as

$$\left.\begin{aligned} E_{za} &= \sum_{n=-\infty}^{\infty} \tilde{A}_n e^{-\alpha_n(x-h/2)} e^{-j\beta_n y}, \\ &\quad h/2 \leqslant x \text{ in air} \\ E_{zf} &= \sum_{n=-\infty}^{\infty} (\tilde{B}_n \cos k_n x + \tilde{C}_n \sin k_n x) e^{-j\beta_n y}, \\ &\quad -h/2 < x < h/2 \text{ in ferrite} \\ E_{zb} &= \sum_{n=-\infty}^{\infty} \tilde{D}_n e^{\alpha_n(x+h/2)} e^{-j\beta_n y}, \\ &\quad -h/2 \geqslant x \text{ in air} \end{aligned}\right\} \tag{5}$$

where

$$\beta_n = \beta + \frac{2\pi n}{d}, \qquad n = 0, \pm 1, \pm 2, \cdots. \tag{6}$$

β is the propagation constant of the dominant space harmonic, and $\tilde{A}_n$, $\tilde{B}_n$, $\tilde{C}_n$, and $\tilde{D}_n$ are unknown expansion coefficients. Substituting (5) into (2), and letting $\epsilon_r = 1$, $\mu_{ef} = 1$ in the air region, we obtain

$$\left.\begin{aligned} k_n &= \sqrt{\omega^2\mu_0\epsilon_0\epsilon_r\mu_{ef} - \beta_n^2}, && \text{in ferrite} \\ \alpha_n &= \sqrt{\beta_n^2 - \omega^2\mu_0\epsilon_0}, && \text{in air} \end{aligned}\right\}. \tag{7}$$

The propagation constant β and unknown coefficients $\tilde{A}_n$, $\tilde{B}_n$, $\tilde{C}_n$, *and* $\tilde{D}_n$ are determined by matching the tangential magnetic and electric fields at $x = \pm h/2$. The required boundary conditions at the interfaces $x = \pm h/2$ are given by

$$H_{yf}(-h/2, y) = H_{yb}(-h/2, y) \tag{8}$$

$$E_{zf}(-h/2, y) = E_{zb}(-h/2, y) \tag{9}$$

$$H_{yf}(h/2, y) - H_{ya}(h/2, y) = J_z(y) = \begin{cases} I_z(y), & \text{on metal strips} \\ 0, & \text{otherwise} \end{cases} \tag{10}$$

$$E_{zf}(h/2, y) = E_{za}(h/2, y) \tag{11}$$

$$E_{zf}(h/2, y) = E_{za}(h/2, y) = 0, \quad \text{on metal strips.} \tag{12}$$

The subscripts f, a, and b denote the fields in the ferrite slab, the above, and the bottom air regions, respectively. $I_z(y)$ in (10) is the unknown surface current density in the z direction on the metal strips. The use of boundary conditions of (8)–(11) allows us to express expansion coefficients $\tilde{A}_n$, $\tilde{B}_n$, $\tilde{C}_n$, and $\tilde{D}_n$ in terms of space harmonics of the surface current density $J_z(y)$. Hence, the relation between the space harmonics of $E_{za}(h/2, y)$ and $J_z(y)$ can be written, after some mathematical manipulations, as

$$\tilde{E}_n = \tilde{G}_n \tilde{J}_n \tag{13}$$

where

$$\tilde{G}_n = j\omega\mu_0 \cdot \frac{\left[\cos k_n h + \dfrac{(\kappa/\mu)\beta_n + \mu_{ef}\alpha_n}{k_n}\sin k_n h\right]}{\left[-2\alpha_n \cos k_n h + \left\{\dfrac{k_n}{\mu_{ef}} + \dfrac{(\kappa/\mu)\beta_n^2}{\kappa_{ef}k_n} - \mu_{ef}\dfrac{\alpha_n^2}{k_n}\right\}\sin k_n h\right]}$$

$$\tilde{J}_n = \frac{1}{d}\int_0^d J_z(y) e^{j\beta_n y}\, dy$$

$$\tilde{E}_n = \frac{1}{d}\int_0^d E_{za}(h/2, y) e^{j\beta_n y}\, dy.$$

$\tilde{J}_n$ and $\tilde{E}_n$ are amplitude coefficients of the nth space harmonic of $J_z(y)$ and $E_{za}(h/2, y)$, respectively. The eigenvalue equation for the propagation constant β can be derived by considering the remaining boundary condition (12). We expand unknown $\tilde{J}_n$ in terms of known sets of basis function $\tilde{J}_{m,n}$ as

$$\tilde{J}_n = \sum_{m=1}^{M} c_m \tilde{J}_{m,n} \tag{14}$$

where c_m is the unknown constant. After substituting (14) into (13), we take scalar products with the basis functions $\tilde{J}_{i,n}^*$ for different values of i ($i = 1, 2, 3, \cdots, M$) and sum over all n. This process leads to the following matrix equation:

$$\sum_{m=1}^{M} G_{im} c_m = \frac{1}{d}\int_0^d E_{za}(h/2, y) J_{z,i}^*(y)\, dy = 0 \tag{15}$$

where

$$G_{im} = \sum_{n=-\infty}^{\infty} \tilde{G}_n \tilde{J}_{m,n} \tilde{J}_{i,n}^*. \tag{16}$$

The integral over a period in (15) is 0, because $E_{za}(h/2, y)$ is 0 on the metal strip and $J_{z,i}(y)$ is chosen to be 0 otherwise. At this step, all the boundary conditions have

been satisfied. The eigenvalue equation for the propagation constant β is now obtained by equating the determinant of the coefficient matrix of (15) equal to 0. That is:

$$\det|G_{im}| = 0. \tag{17}$$

The accuracy of the solution of (17) depends on the choice of the basis function $J_{z,m}(y)$ [4]. In this paper, the following form has been chosen:

$$J_{z,m}(y) = \begin{cases} \cos\dfrac{2(m-1)\pi}{s}y, & 0 \leqslant y \leqslant s \\ 0, & s \leqslant y \leqslant d. \end{cases} \tag{18}$$

The basis function $J_{z,m}(y)$ is nonzero only on the metal strips.

III. Numerical Results

The dispersion relation is obtained by evaluating numerically the root of the eigenvalue equation (17). Before presenting the numerical results of the dispersion relation in the ferrite slab with periodic metal strips, it is desirable to describe the propagation properties of waves in the ferrite slab without metal strips. The dispersion relation for the TE modes of the transversely magnetized ferrite slab is given by [6]

$$\left(\frac{k^2}{\mu_{ef}^2} + \frac{\beta^2}{\kappa_{ef}^2} - \alpha^2\right)\tan kh - \frac{2\alpha k}{\mu_{ef}} = 0 \tag{19}$$

which is also obtained by setting the denominator of $\tilde{G}_n$ equal to 0, where k and α are determined from (7) with $n = 0$. The solution β of (19) for a given frequency f includes volume waves and surface waves. Fig. 2 shows the dispersion diagrams of these TE waves in a ferrite slab for the bias magnetic-field strength of 10 kG. Within the frequency band $f_1[=\gamma\mu_0\sqrt{H_0(H_0+M)}/2\pi] < f < f_2[=\gamma\mu_0(H_0+M)/2\pi]$ and for $\beta > \omega\sqrt{\mu_0\epsilon_0\epsilon_r\mu_{ef}}$, k is imaginary and only surface waves corresponding to magnetostatic and dynamic surface modes, discussed in detail by Gerson and Nadan [6], can exist. Outside these frequency regions, dispersion curves for the volume waves exist in the high- and the low-frequency region because k is real where $\omega\sqrt{\mu_0\epsilon_0} < \beta < \omega\sqrt{\mu_0\epsilon_0\epsilon_r\mu_{ef}}$.

When periodic metal strips are provided, the dispersion relation of (17) is calculated numerically, particularly around the first-order Bragg interaction regions A, B, and C of Fig. 2. The result is shown in Fig. 3, where the parameter values used in the calculation are also given. The important feature is that the stopbands in frequency occur where the Bragg condition

$$\mathrm{Re}(\beta^+ + \beta^-) = 2\pi/d \tag{20}$$

is satisfied. The superscripts "+" and "−" indicate the forward and backward wave, respectively. The stopbands at A and C result from the interaction between the dominant space harmonic ($n = 0$) of forward volume waves and the dominant space harmonic ($n = -1$) of backward volume waves. The stopband at B results from the interaction between the forward wave of the dynamic surface

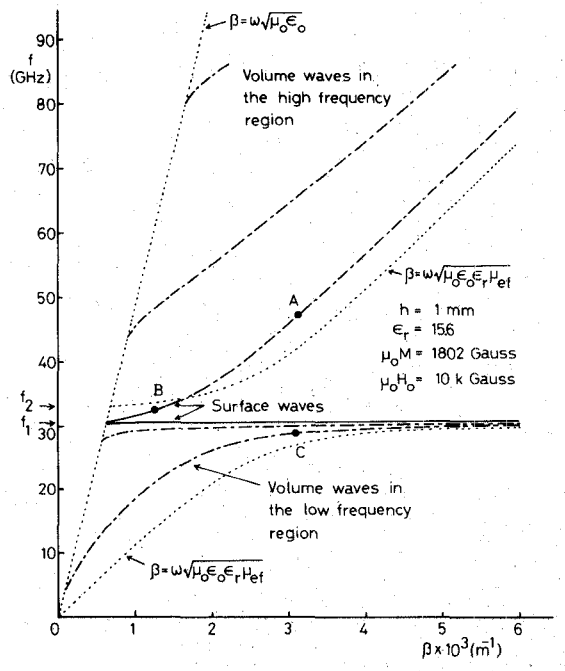

Fig. 2. Dispersion diagram for the TE mode of the ferrite slab without metal strips.

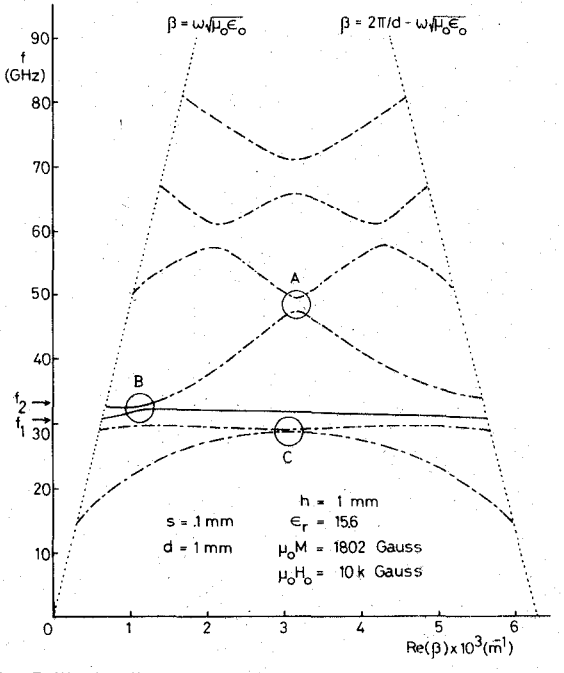

Fig. 3. Brillouin diagram for the TE mode of the ferrite slab with periodic metal strips.

mode and the backward wave of the magnetostatic surface mode. In the calculation of the Brillouin diagram of Fig. 3, summation up to $n = \pm 50$ of the space harmonics and matrix size $M = 2$ in (17) have been used. The convergence of the solutions of (17) has also been checked for various sizes of matrix, and we have found that good results are obtained even for $M = 1$. Fig. 4(a), (b), and (c) shows the enlarged Brillouin diagrams in the vicinity of the interaction points A, B, and C, respectively. The propagation constant β is complex in these stopband regions. It is

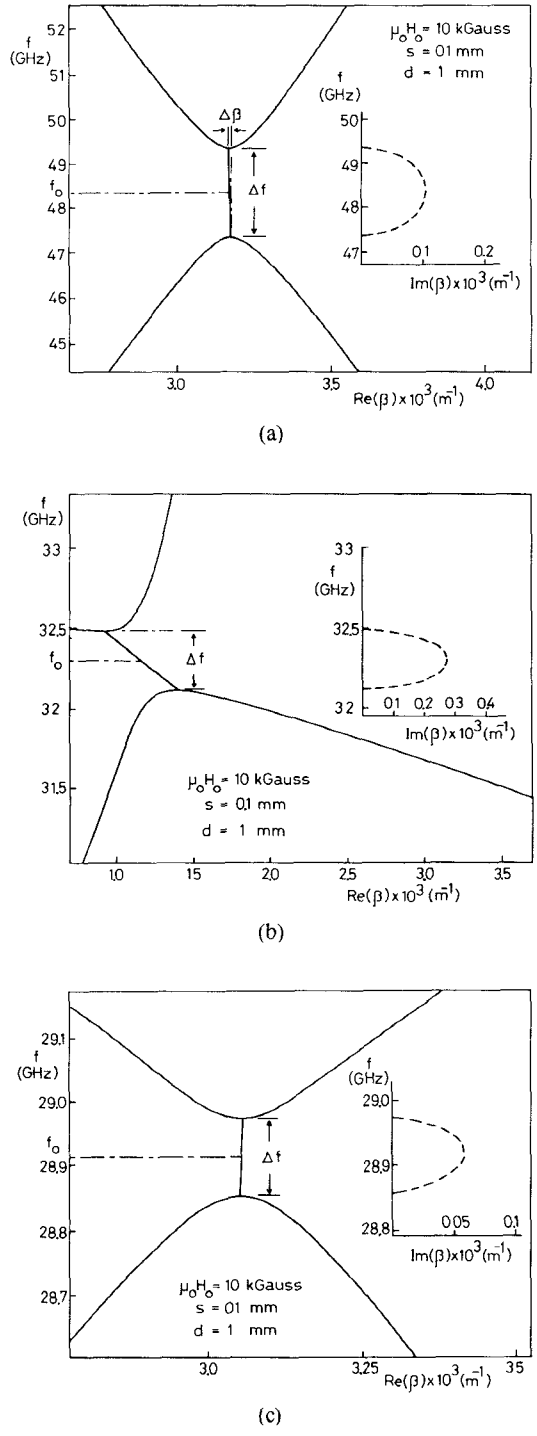

Fig. 4. Enlarged Brillouin diagram in the vicinity of the first-order Bragg interaction regions: (a) at interaction point A, (b) at interaction point B, and (c) at interaction point C.

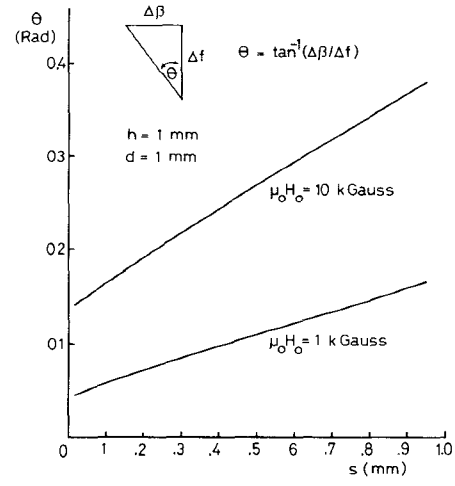

Fig. 5. Computed θ value as a function of strip width for the Bragg interaction of the lowest order volume waves in the high-frequency region.

noted that the attenuation constant Im(β) of the stopband at point B is several times larger than those at points A and C. This property may be useful for designing the band-rejection filters of the microwave frequency. The Brillouin diagrams in Fig. 4 are asymmetric in form, in particular for the surface wave. This is because the metal strips perturb the waveguide structure in an asymmetric way and create the nonreciprocal effect to waves propagation in the forward and backward directions [6]. The nonreciprocal properties can also be explained in connection with (13) and (17). The linear term in κ of (1) and β_n appears in $\tilde{G}_n$ of (13). Therefore, the solutions of the eigenvalue equation (17) have nonreciprocal characteristics. The wave interactions are asymmetric, with the consequence that the propagation constant varies as a linear function of frequency in the stopband region. The angle of the slope that the propagation constant makes to the frequency axis within the stopband region, $\theta = \tan^{-1}(\Delta\beta/\Delta f)$, will be used here as a parameter to show the existence of the nonreciprocal behavior of waves. To determine the effects of the stripwidth on the nonreciprocal behavior of waves, for example, for the Bragg interaction of the lowest order volume waves in the high-frequency region of Fig. 4(a), dependence of θ at point A on the stripwidth is numerically evaluated as a function of bias magnetic field and is plotted in Fig. 5. It is found that θ, and hence the nonreciprocity of volume waves in the high-frequency region, increases with increasing both the stripwidth and bias magnetic-field strength.

IV. Experimental Results

Experiments on the Bragg reflection characteristics have been carried out in the 40–50-GHz frequency region. The Bragg frequency is chosen to be at the interaction point A of Fig. 3. Two polycrystalline YIG slabs with finite linewidth of 75 Oe are used as the guiding layer. Dimensions of both slabs are 15 mm wide, 1 mm thick, and 100 mm long. Periodic metal strips are created on the slab surface by sticking 35-μm-thick and 0.4-mm-wide copper strips at a period of 1 mm for sample 1 and by depositing (by vacuum evaporation) 10-μm-thick and 0.1-mm-wide gold strips at a period of 1 mm for sample 2. The number of metal strips for sample 1 is 65 and for sample 2 is 60. Both ends of the slab are tapered and the absorber is coated at the far end when Bragg reflection characteristics are measured. A bias-dc magnetic field is applied parallel to the slab surfaces and perpendicular to the direction of propa-

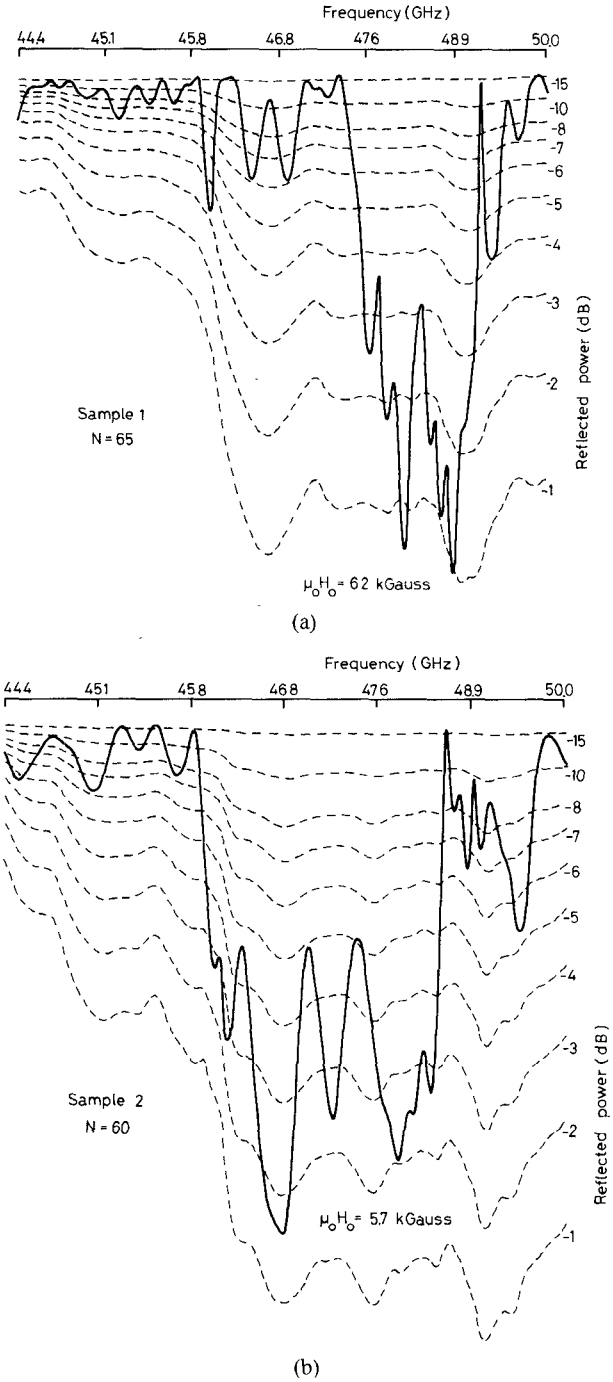

Fig. 6. Typical Bragg reflection characteristics as a function of frequency: (a) for sample 1 with $N = 65$ and (b) for sample 2 with $N = 60$.

gation by an electromagnet. The measurement setup is similar to that employed in the measurement of Bragg reflection from a corrugated ferrite slab [1]. The TE wave in the slab is excited from a WRI-500 rectangular waveguide diretly or by using an electromagnetic horn antenna. A reflected wave is selectively detected through the directional coupler. Fig. 6(a) and (b) shows the measured Bragg reflection characteristics from sample 1 for the bias magnetic-field strength of 6.2 kG and sample 2 for the bias magnetic-field strength of 5.7 kG, respectively. The 3-dB

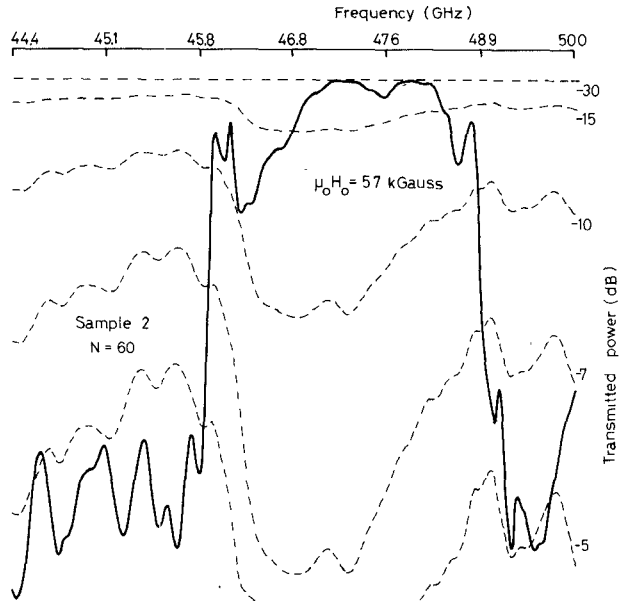

Fig. 7. Transmission characteristics as a function of frequency for sample 2 with $n = 60$.

bandwidth as measured for sample 1 is about 2.1 GHz with return loss about 1.5 dB at the Bragg frequency of 48.68 GHz. For sample 2, the 3-dB bandwidth is about 2.14 GHz with return loss about 2 dB at the Bragg frequency of 47.5 GHz. Transmission characteristics of sample 2 are also measured and are shown in Fig. 7 for the bias magnetic-field strength of 5.7 kG. The stopband in frequency between 46 and 48.9 GHz confirms the corresponding stopband response of the reflection characteristics of Fig. 6(b). From Fig. 7, it is seen that the difference in power level between the power level at the Bragg frequency and the spurious level is more than 23 dB. The measured magnetic-field dependence of the Bragg frequency f_0 and 3-dB bandwidth Δf for sample 1 and 2 are plotted in Fig. 8(a) and (b). Theoretical results obtained from the Brillouin diagram of Fig. 4(a) are also depicted in the figure by the solid lines. The values in the ordinate scale for the Bragg frequency are normalized to the values at zero-bias magnetic field, which are 46.65 GHz (sample 1) and 46.17 GHz (sample 2), theoretically, and 47.69 GHz (sample 1) and 46.85 GHz (sample 2), experimentally. It is seen that the normalized f_0 values of the experimental results for both sample 1 and 2 agree well with the computed results. The measured Bragg frequency for sample 1 and 2 can be tuned over the range of 1.26 and 1.39 GHz by varying bias magnetic-field strength from 0 to 7.2 kG and 8.2 kG, respectively. The measured 3-dB bandwidths for sample 1 are about 25 percent narrower than the computed results, but for sample 2 they are in good agreement with the computed ones. The difference between the theory and experiment of the Δf values for sample 1 seems to be due to the effects of the adhesives between the strips and slab surface, and the fabrication irregularity of the strips in the experiment. It is noted that the stop bandwidth is nearly unvaried over the range of the applied bias magnetic-field strength.

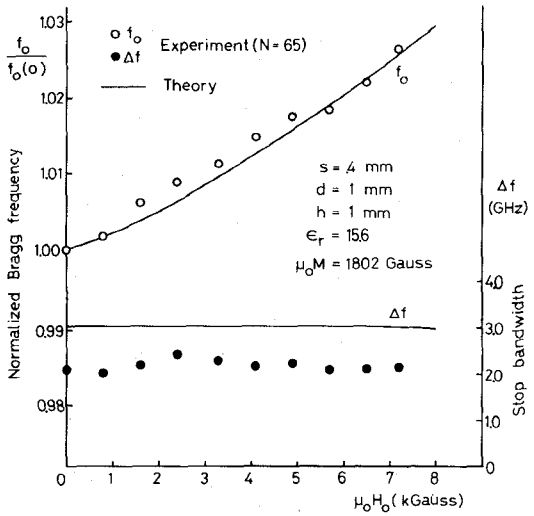

(a)

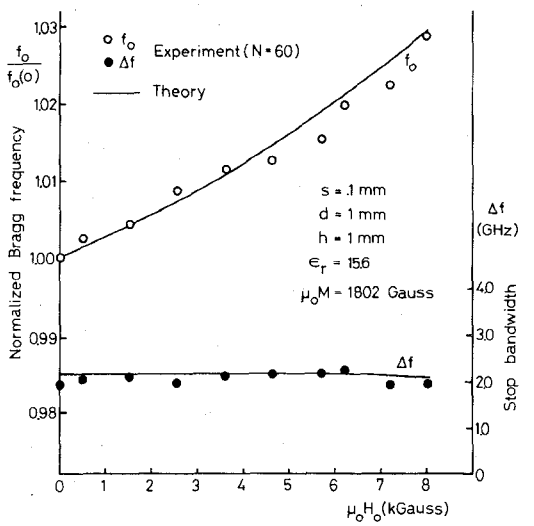

(b)

Fig. 8. Measured and computed magnetic-field dependence of the Bragg frequency and stop bandwidth: (a) for sample 1 and (b) for sample 2.

V. Conclusion

The propagation characteristics of TE waves in a ferrite slab periodically loaded with metal strips are investigated by the spectral domain approach. Stopband and nonreciprocal properties of the volume and surface waves in the waveguide structure are characterized by the bias magnetic-field strength. It is noted that the attenuation constant of the surface mode is several times larger than that of the volume modes. Experiments on the Bragg reflection have been carried out in the millimeter-wave frequencies using two polycrystalline YIG slabs periodically loaded with copper and gold strips, respectively. Typical results obtained for sample 1 are stop bandwidth about 2.1 GHz with return loss about 1.5 dB at the Bragg frequency of 48.68 GHz for the bias magnetic-field strength of 6.2 kG, and for sample 2 are stop bandwidth about 2.14 GHz with return loss about 2 dB at the Bragg frequency of 47.5 GHz for the bias magnetic-field strength of 5.7 kG The Bragg frequency for samples 1 and 2 can be tuned over the range of 1.26 and 1.39 GHz by varying the bias magnetic field from zero to 7.2 and 8.2 kG, respectively. Experimental results agree well with the numerical results.

The ferrite slab with periodic metal strips can be easily and accurately fabricated when compared with the surface-corrugated ferrite slab [1], and has tunable Bragg reflection characteristics. It seems to be useful for applications in the tunable band-rejection filters or electronically steerable leaky-wave antenna [7] in the microwave and millimeter-wave frequencies.

References

[1] M. Tsutsumi and N. Kumagai, "Bragg reflection of millimeter waves by a corrugated ferrite slab", *J. Appl. Phys.*, vol. 53, pp. 5959–5963, Aug. 1982.

[2] T. Ohira, M. Tsutsumi, and N. Kumagai, "Radiation of millimeter waves from a grooved ferrite image line", *Proc. IEEE*, vol. 70, pp. 682–683, June 1982.

[3] K. Araki and T. Itoh, "Analysis of periodic ferrite slab waveguides by means of improved perturbation method", *IEEE Trans. Microwave Theory Tech.*, vol. MTT-29, pp. 911–916, Sept. 1981.

[4] K. Ogusu, "Propagation properties of a planar dielectric waveguide with periodic metallic strips", *IEEE Trans. Microwave Theory Tech.*, vol. MTT-29, pp. 16–21, Jan. 1981.

[5] B. Lax and K. J. Button, *Microwave Ferrite and Ferrimagnetics*. New York: McGraw-Hill, 1962, p. 145.

[6] T. J. Gerson and J. S. Nadan, "Surface electromagnetic modes of a ferrite slab", *IEEE Trans. Microwave Theory Tech.*, vol. MTT-22, pp. 757–762, Aug. 1974.

[7] R. E. Horn, H. Jacobs, E. Freibergs, and K. L. Klohn, "Electronic modulated beam-steerable silicon waveguide array antenna", *IEEE Trans. Microwave Theory Tech.*, vol. MTT-28, pp. 647–653, June 1980.

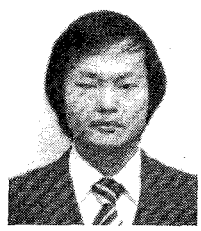

Charray Surawatpunya was born in Bangkok, Thailand, on June 6, 1953. He received the B. E. degree in telecommunication engineering with First Class Honors from King Mongkut's Institute of Technology, Ladkrabang Campus, Bangkok, Thailand, in 1977. Since 1978, he has continued his graduate studies at Osaka University, Japan, as a recipient of the Monbusho Scholarship from the Japanese Government. He received the M. E. degree in communication engineering in 1981 and will receive the Ph.D. degree in March, 1984.

His research interests are mainly in millimeter-wave integrated circuits and components.

Makoto Tsutsumi (M'71) was born in Tokyo, Japan, on February 25, 1937. He received the B.S. degree in electrical engineering from Ritsumeikan University, Kyoto, in 1961, and the M.S. and Ph.D. degrees in communication engineering from Osaka University, Osaka Japan, in 1963 and 1971, respectively.

He has been a Lecturer in the Department of Communication Engineering, Osaka University. His current research areas include microwave and millimeter-wave ferrite devices.

Dr. Tsutsumi is a member of the Institute of Electronics and Communication Engineers of Japan and Japan Society of Applied Physics.

Nobuaki Kumagai (M'59–SM'71–F'81) was born in Ryojun, Japan, on May 19, 1929. He received the B. Eng. and D. Eng. degrees from Osaka University, Osaka, Japan, in 1953 and 1959, respectively.

From 1956 to 1960, he was a Research Associate in the Department of Communication Engineering at Osaka University. From 1958 through 1960, he was a Visiting Senior Research Fellow at the Electronics Research Laboratory of the University of California, Berkeley, while on leave of absence from Osaka University. From 1960 to 1970, he was an Associate Professor, and has been a Professor of Communication Engineering at Osaka University since 1971. He served as a Department Chairman in the periods of 1972–1973, 1977–1978, and 1983–1984. From 1980 to 1982, he was the Dean of Students of Osaka University.

His fields of interest are electromagnetic theory, microwaves, millimeter waves, and acoustic-waves engineering, optical fibers and optical fiber communication techniques, optical integrated circuits and devices, and lasers and their applications. He has published more than 100 technical papers on these topics in established journals. He is the author or coauthor of several books including *Microwave Circuits* and *Introduction to Relativistic Electromagnetic Field Theory*. From 1979 to 1981, he was Chairman of the Technical Group on the Microwave Theory and Techniques of the Institute of Electronics and Communication Engineers of Japan. He is chairman of the Kinki Regional Broadcast Program Council of the Japan Broadcasting Corporation (NHK), and is the consultant for the Nippon Telegraph and Telephone Public Corporation (NTT).

Dr. Kumagai is a member of the Institute of Electronics and Communication Engineers of Japan, the Institute of Electrical Engineers of Japan, and the Laser Society of Japan. He was awarded an IEEE Fellowship for contributions to the study of wave propagation in electromagnetics, optics, and acoustics.

Design of Waveguide *E*-Plane Filters with All-Metal Inserts

YI-CHI SHIH, MEMBER, IEEE

Abstract—**Waveguide *E*-plane filters with all-metal inserts are designed by a procedure based on the reflection coefficients of axial inductive strips. The scattering matrix, representing the junction in a bifurcated waveguide, is calculated by a mode-matching method. The reflection coefficient for an inductive strip is then obtained by cascading two scattering matrices separated by a distance equal to the stripwidth. The design is valid up to moderate bandwidths, except for the narrowband design at the higher waveguide frequency range, where both the center frequency and the bandwidth are inaccurate. Possible sources of error are studied and a method minimizing the error is proposed.**

I. Introduction

WAVEGUIDE *E*-plane filters with all-metal inserts (Fig. 1) were originally proposed as low-cost mass-producible circuits for microwave frequencies [1], [2]. More recently, they have been designed for millimeter-wave applications through computer-optimization routines based on accurate analyses [3], [4]. The *E*-plane circuit is developed on a metal sheet by photo-etching, pressing, or stamping. The widths of the slot patterns on the metal sheet are equal to the waveguide height; thus, after assembly, the structure consists of several resonators separated by axial inductive strips. Because dielectric losses are absent, the structure has a high transmission Q factor and is suitable for narrow-band high-Q applications.

Manuscript received November 14, 1983; revised February 27, 1984. This work was supported by the Naval Postgraduate School Foundation Research Program.

The author is with the Electrical Engineering Department, Naval Postgraduate School, Monterey, CA 93943.

In computer-aided designs [3], [4], the optimization program finetunes the filter circuit to make the filter performance satisfy a set of specifications. This feature is desirable in millimeter-wave applications because physically finetuning a circuit of small size is a difficult task. With the aid of the optimization program, human effort is minimized in the process of design. The drawback is, however, the expensive computer resources required for each design. Compared with computer optimization, the network synthesis procedures described in [1] and [2] require only minimum computer time to design a filter. In [1], the procedure is based on a low-pass prototype, and therefore gives good results for narrowband design only. In [2], the procedure is based on a distributed prototype and can be used up to a relatively wide bandwidth; it requires, however, several iterations to complete a design. Unlike the optimization program, which is based on an accurate analysis, the synthesis procedure involves some approximations. Although the design examples given in [1] and [2] have been shown to be valid, there is no guarantee that other designs will be valid. It is, therefore, the purpose of this paper to introduce a design procedure with which one can design an *E*-plane filter up to moderate bandwidth and still have confidence in the result.

The design procedure, based on a distributed step-impedance filter prototype, is a modified version of that described by Levy [5] for design of direct-coupled-cavity filters. For a given set of filter specifications, the junction reflection coefficients at the discontinuities are calculated

0018-9480/84/0700-0695$01.00 ©1984 IEEE